

Spectroscopic measurement of temperature and gas composition in Ar-N₂ shielded TIG welding

Xiao Xiao^{1,2,3} · Xueming Hua^{1,2} · Fang Li^{1,2} · Yixiong Wu^{1,2}

Received: 21 May 2015 / Accepted: 11 July 2016 / Published online: 29 July 2016
© International Institute of Welding 2016

Abstract Demixing causes changes in the composition and thermal transport in a mixed-gas arc. Thus, the temperature and gas composition of argon–nitrogen arc plasma are measured to analyze the effect of demixing in both direct-current tungsten inert gas (DC-TIG) and pulsed TIG (P-TIG) welding. The arc image acquisition system is developed; this system includes two monochromatic imaging devices, which are triggered synchronously by software. The presented system is an efficient approach to capture monochromatic images simultaneously with high temporal and spatial resolutions. It is applied to obtain monochromatic images of the Ar I and N I spectra. Using the modified Fowler–Milne method, the radial profiles of temperature and gas composition are measured. For DC-TIG in 80 % Ar + 20 % N₂, the argon concentration is decreased in the arc centre, relative to the original gas mixture, and then gradually increases with the radius. This is attributed to frictional forces. As the radius increases further, the argon mass fraction decreases again,

which is attributed to diffusion of argon toward the arc periphery. For P-TIG using 80 % Ar + 20 % N₂, the demixing effect in the peak-current phase is stronger than that in the base-current phase due to the higher current in the peak-current phase. This phenomenon helps control the heat input into the workpiece.

Keywords (IIW Thesaurus) GTA welding · Arc physics · Mixtures · Shielding gases · Imaging

1 Introduction

Using proper shielding gases in tungsten inert gas (TIG) welding can improve efficiency and reduce cost; thus, various gas mixtures have been used. For example, argon and nitrogen mixtures of certain compositions are often used in welding copper [1] and stainless steel [2]. However, demixing often causes a change in the composition of this type of arc plasma during welding [3], thereby influencing the thermal transport and even the physical property of the arc plasma. This paper focused on the measurement of the temperature and gas composition of argon–nitrogen arc plasma to obtain a better understanding of the mechanism of mixed-gas welding.

As a non-invasive diagnostic method, optical emission spectroscopy has been widely used in arc plasma measurement. Spectroscopic methods can be divided into two groups according to the required equipment: spectrometer and monochromatic imaging. Over the past decades, spectrometers have been extensively used to measure the spectral intensities of both single-element [4] and multi-element [5] arc plasmas. In the spectrometer-based method, the arc plasma is scanned point by point; thus, the spatial resolution is low, and the time required to

Recommended for publication by Study Group 212 - The Physics of Welding

✉ Xueming Hua
xmhua@sjtu.edu.cn

¹ Shanghai Key Laboratory of Materials Laser Processing and Modification, School of Materials Science and Engineering, Shanghai Jiao Tong University, Shanghai 200240, People's Republic of China

² Collaborative Innovation Center for Advanced Ship and Deep-Sea Exploration, Shanghai 200240, People's Republic of China

³ School of Materials Science and Engineering, Henan University of Science and Technology, Luoyang 471023, People's Republic of China

complete the measurement is long. Thus, the application of this method is limited to the measurement of steady-state arc plasma, whereas the dynamic changes in the entire arc plasma are difficult to investigate using this method. By contrast, monochromatic imaging is an efficient method for measuring the spectral intensities in high temporal and spatial resolutions, and a relatively simple route to obtain two-dimensional images is to use a narrow bandpass filter with an imaging detector. However, given that each imaging detector only collects information from a narrow spectral region, the reduced amount of data limits the analyses that can be performed; consequently, the method has not been applied often to TIG welding arcs. Ma measured the temperature of pure argon arc plasma by this method in both pulsed TIG (P-TIG) [6] and direct-current TIG (DC-TIG) welding, which included steady state [7] and arc ignition [8]. Sawato [9] also used this method in P-TIG welding at different currents. Their studies proved that the monochromatic imaging method showed good temporal and spatial resolutions. However, the application of this method to multi-element arc plasma is restricted, because this method only acquires one spectral intensity, which is insufficient to determine the temperature and gas composition in multi-element arc plasma. Recently, our group [10] used this method to measure Ar–He arc plasma in DC-TIG welding and found a slight fluctuation in temperature and a change in gas composition after arc ignition. However, the spectral intensities were not obtained simultaneously; thus, a double monochromatic imaging system should be developed to improve its accuracy.

Over the past years, a number of studies have focused on characterizing the arc properties of multi-element plasma by different methods. Song Yonglun et al. used the absolute intensity method to measure argon–hydrogen arc plasma [11] and argon–nitrogen arc plasma [12]. Hiraoka used the two-line intensity correlation method for Ar–He [13] or Ar–H₂ [14] mixed-gas tungsten arc

plasma. These methods allow for the simple measurement of the temperature and composition of arc plasma. However, they require spectroscopic data, such as transition probability. The values reported in the literature [15] significantly vary, causing errors in the calculation. Murphy [16] used a modified Fowler–Milne method to measure the radial profiles of the temperature and gas composition of the argon and nitrogen mixtures. This method does not require the frequent calibration of test apparatus and knowledge of the atomic transition probability. This method can also allow for a more precise derivation of the relative concentrations of gas elements than other spectroscopic methods [16]. Xiao et al. [17] modified the Fowler–Milne method and analyzed the error distribution of the Ar–He arc plasma; they reported that the developed Fowler–Milne method had a relatively small error. Accordingly, the modified Fowler–Milne method was used in the current paper.

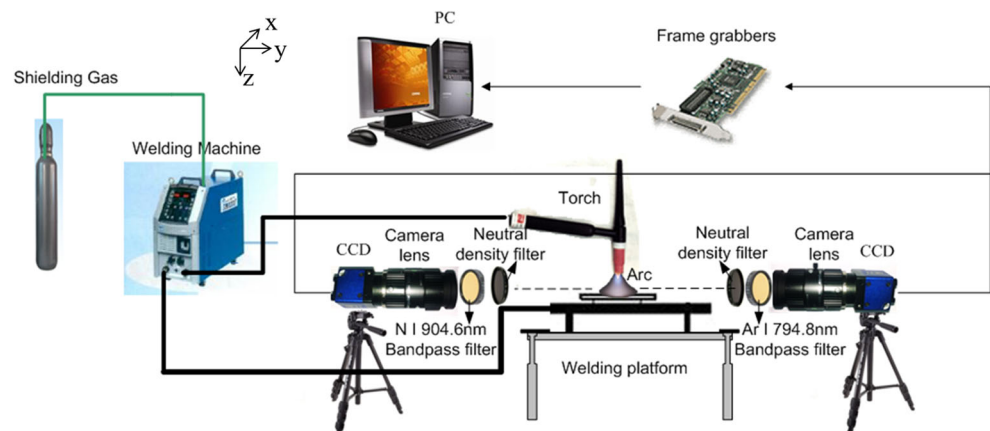
In this study, a monochromatic imaging system was used to obtain monochromatic images, and the modified Fowler–Milne method was used to measure the temperature and gas composition of the argon–nitrogen arc plasma in TIG welding. The experimental system is described in Section 2. Section 3 explains the modified Fowler–Milne method and data processing with monochromatic arc images. Section 4 presents the measurement and analyses of the distributions of temperature and gas composition in both static (DC-TIG) and dynamic (P-TIG) states. Section 5 presents the conclusions.

2 Experimental details and procedures

2.1 Arc plasma source

The schematic diagram of the experimental system is shown in Fig. 1. The arc was struck between the tungsten cathode and the copper plate anode by a welding power

Fig. 1 Schematic diagram of the synchronous arc image acquisition system



supply (OTC-DA300P). The cathode was a thoriated tungsten rod (diameter 2.4 mm), which is ground to a conical tip with a 60° angle. The anode was a water-cooled copper plate, which does not melt during welding; as a result, the metal vapor did not significantly influence the temperature distribution [18] and the gas composition distribution was measured more precisely. The distance between the anode and the cathode was 5 mm. The nitrogen concentration was usually maintained low to avoid nitrogen porosity [12]. The shielding gas, which was a mixture of argon (80 % in volume) and nitrogen (20 % in volume), was fed from the cathode nozzle at a flow rate of 10 L min⁻¹, and the electric current was 200 A.

2.2 Synchronous arc image acquisition system

Radiations from the arc were measured by two monochromatic imaging devices, which were triggered synchronously by a software program. They were located on both sides of the arc plasma and perpendicular to the arc. Each of the monochromatic image devices was composed of neutral density filters, a narrow bandpass filter, a camera lens, and a CCD sensor (Fig. 1). The camera lenses (M7528-MP, Daheng Imavision) were placed 0.5 m away from the arc. The narrow bandpass filters were mounted before the camera lenses in this test to record the spectral line intensity. The narrow bandpass filter of one CCD sensor was Ar I 794.8 nm with 3 nm full width at half maximum (FWHM), and that of the other CCD sensor was N I 904.6 nm with 7 nm FWHM. As a consequence of placing neutral density filters in front of the narrow bandpass filters and carefully tuning the apertures of the camera lenses, the strong radiation from the arc was reduced and an unsaturated image with proper intensity was

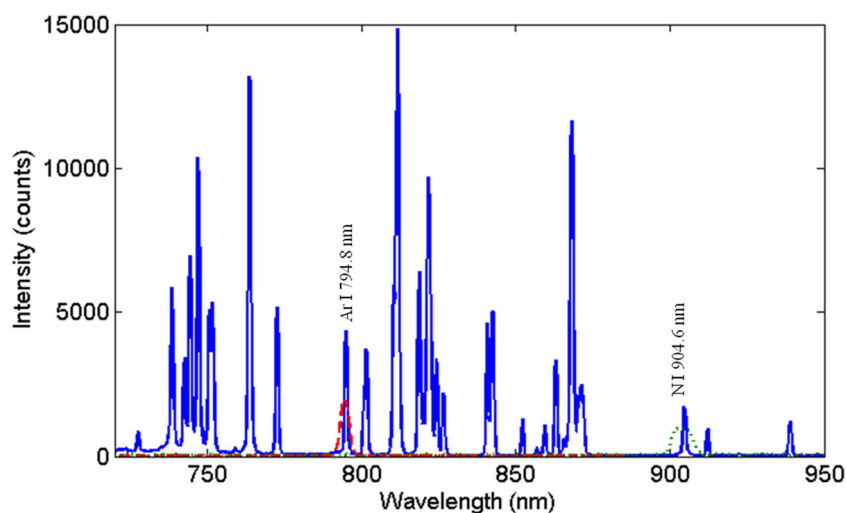
obtained. The camera (acA1600-20gc, Basler) was capable of capturing 8-bit gray images (500 × 400 pixels of the CCD sensor) at a frame rate of 20 Hz after the images passed through the filters and lenses.

The arc spectra were recorded with a spectrometer before the experiment to allow for the selection of the spectral lines. By spectroscopic measurement, we found that the Ar I and N I spectral lines appeared at different positions of the arc. Figure 2 shows the 750–950-nm arc spectrum measured in the column region of the arc at a distance of 2 mm below the cathode tip; it contains the Ar I and N I spectral lines. Therefore, the Ar I 794.8 nm line and N I 904.6 nm line were used to characterize the plasma properties. These lines were selected because they were well separated from other lines, and their intensities were acceptably large. The short dashed line and dashed line in Fig. 2 show the transmittance curves of the narrow bandpass filters. For the experimental system, the images captured the intensities of the Ar I 794.8 nm line and the N I 904.6 nm line, as well as the continuum near them.

3 Measurement and data processing

The plasma fluctuations and experimental component noises served as interferences on the side-on measured spectral line intensity; thus, its intensity profile needs to be noise filtered and symmetrized to improve the accuracy of the measurement. The continuum radiation is ignored, because its intensities for both Ar I 794.8 nm and N I 904.6 nm in the spectrum are very weak, particularly if compared with their spectral lines. Subsequently, the intensity distribution is converted into emission coefficients by using Abel inversion, provided

Fig. 2 Spectrum distribution between 750 and 950 nm (*blue line*) and the transmittance curve of two narrow bandpass filters in a 200-A free-burning arc with 80 % Ar + 20 % N₂ shielding gas



the plasma is cylindrically symmetrical and optically thin. The Bockasten method [19], which is easy to operate and has minimal error, is used to accomplish Abel inversion.

The spectral emission coefficient, ε_{nm} , of the transition from level m to lower level n of species j in a plasma is expressed as [20]

$$\varepsilon_{nm} = \frac{hc}{4\pi\lambda_{nm}} g_m A_{nm} \frac{n_j(T, Y)}{U_j(T, Y)} \exp\left(-\frac{E_m}{kT}\right), \quad (1)$$

where Y is the mole fraction of argon, that is, the gas composition; $n_j(T, Y)$ and $U_j(T, Y)$ are the number density and the partition function of species j at Y mole fraction, respectively; λ_{nm} is the wavelength of the spectrum; g_m and E_m are the statistical weight and energy of the upper level; A_{nm} is the transition probability; and h , c , and k are Planck's constant, the speed of light, and Boltzmann's constant, respectively.

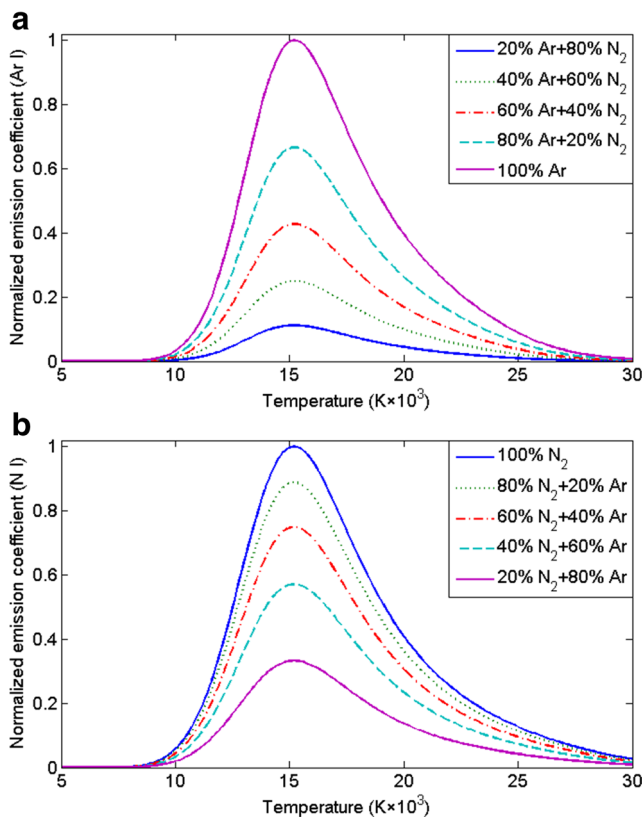


Fig. 3 Dependencies of the emission coefficient of **a** the 794.8 nm Ar I line and **b** the 904.6 nm N I line on temperature, normalized to its maximum value in pure arc, for different mixtures of argon and nitrogen

For the argon–nitrogen arc plasma, the normalized emission coefficient of the Ar I 794.8 nm line and the N I 904.6 nm line depends both on temperature and composition, and it could be calculated from Eq. 1 for different ratios and normalized to their respective maximum values in pure arc plasma. The curves showing the relationship between temperature and the normalized emission coefficients of Ar I and N I are shown in Fig. 3.

However, a value of the normalized emission coefficient of either the Ar I 794.8 nm line or the N I 904.6 nm line corresponds to an infinite number of temperature–mole fraction pairs. Therefore, each normalized emission coefficient, ε_{ArI} , of the Ar I 794.8 nm line corresponds to a curve $Y(T, \varepsilon_{ArI})$; likewise, each value of ε_{NI} of the N I 904.6 nm line corresponds to a curve $Y(T, \varepsilon_{NI})$, where Y is the mole fraction of argon. These dependencies are shown in Fig. 4, which shows Y plotted against temperature, T , for different values of ε_{ArI} and ε_{NI} . If both ε_{ArI} and ε_{NI} are known, then the number of corresponding temperature–mole fraction pairs is, at most, two. As in the single-element case, the temperature (and thus the mole fraction value) is generally selected by assuming it increases toward the arc axis. The measurement of the temperature and gas composition of nitrogen–argon plasma require both ε_{ArI} and ε_{NI} , which have to be normalized to their corresponding maximum values in pure argon and pure nitrogen arcs, respectively. This procedure is the modified Fowler–Milne method.

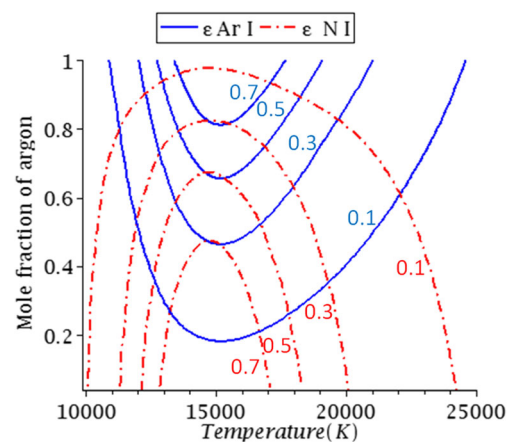
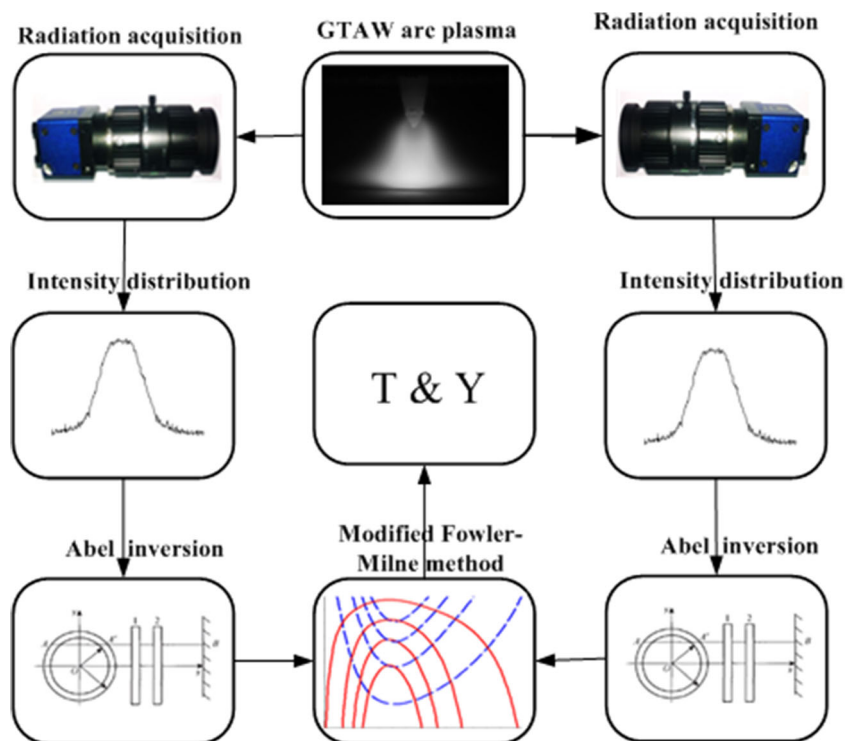


Fig. 4 Relationship between the mole fraction of argon and temperature for different normalized emission coefficients in argon–nitrogen shielding gas. *Solid lines* correspond to different values for Ar I 794.8 nm, and *dotted lines* correspond to different values for N I 904.6 nm

Fig. 5 Principle of data processing in the two-element Fowler–Milne method



The general principle of data processing in the modified Fowler–Milne method is shown in Fig. 5. The intensities of both the Ar I and N I lines are obtained through the arc images simultaneously captured by the synchronous arc image acquisition system, converted into emission coefficients by Abel inversion, and then normalized to their corresponding maximum emission coefficients in pure argon and pure nitrogen, respectively; after the normalized emission coefficients are obtained, the arc temperature and gas composition are determined using the modified Fowler–Milne method [16].

4 Results and discussion

Panels a and b of Fig. 6 show the arc images of Ar I 794.8 nm in pure argon and N I 904.6 nm in pure nitrogen, respectively. In the experimental system, the normalized emission coefficient of the Ar I 794.8 nm line corresponds to the off-axis maximum value in Fig. 6a; likewise, the normalized emission coefficient of the N I 904.6 nm line corresponds to the off-axis maximum value in Fig. 6b. Panels c and d of Fig. 6 show the arc images of Ar I 794.8 nm and N I 904.6 nm, respectively, in the 80 % argon + 20 % nitrogen mixture; their emission coefficients are normalized to their respective maximum values in their pure gas.

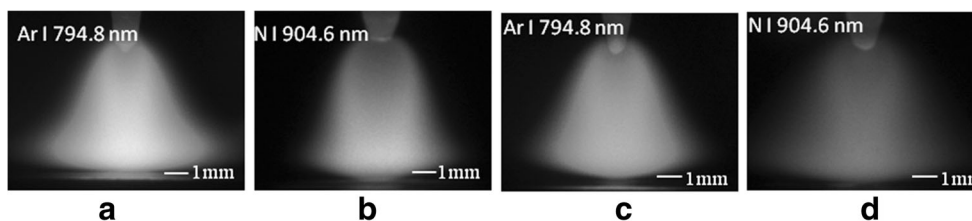


Fig. 6 Arc images of **a** Ar I 794.8 nm in pure argon, **b** N I 904.6 nm in pure nitrogen, **c** Ar I 794.8 nm with input gas 80 % Ar + 20 % N₂, and **d** N I 904.6 nm with input gas 80 % Ar + 20 % N₂ in a 200-A free-burning arc

As a typical example, Fig. 7a shows the arc intensity measured 2 mm below the cathode in the argon–nitrogen arc. The intensity of the Ar I line is higher than that of the N I line given the high argon content of the arc plasma. The corresponding normalized emission coefficients are presented in Fig. 7b. The Ar I line shows an off-axis maximum value at a lateral position of approximately 1 mm, whereas the N I line shows a maximum value at the axis position. This result is associated with the demixing phenomenon. When demixing occurs, a higher concentration increases the emission coefficient.

The radial profiles of the values of the plasma temperature and composition inferred from the emission coefficients are shown with the error bars in Fig. 8a, b. The errors in temperature and mass fraction are between ± 1.52 and ± 1.96 %, which are calculated according to the error transfer formula [17]. The relatively low errors are attributed to the suitability of the modified Fowler–

Milne method [16] and the good spatial resolution of the experimental system.

The radial profiles of the temperature and gas composition of the 80 % Ar + 20 % N₂ arc plasma at distances of 1–4 mm from the cathode tip are presented in Fig. 9a, b. The temperature decreases as the point moves away from the axis along the radial direction but increases as the point approaches the cathode. Under the same experimental condition, the temperature of the 80 % Ar + 20 % N₂ arc plasma is higher than that of the pure argon arc plasma [20]. This result indicates that demixing results in a minimal increase in the heat flux [3]. The mass fraction of argon increases as the radius increases up to 2 mm; this effect is chiefly a result of demixing due to frictional forces. Such demixing can act in different directions depending on the composition of the argon–nitrogen mixture; when the mole fraction of nitrogen is low, such as in the 80 % Ar + 20 % N₂ mixture, the demixing causes an increase in the nitrogen concentration [3]. Thus, the mass

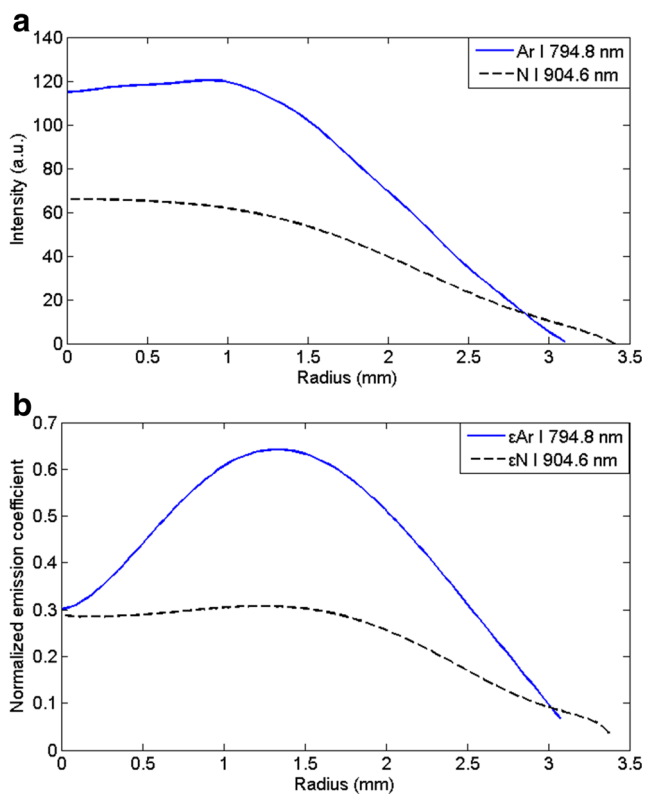


Fig. 7 Radial dependencies of **a** intensity and **b** normalized emission coefficients ε_{ArI} for Ar I 794.8 nm line and ε_{NI} for N I 904.6 nm line, measured 2 mm below the cathode with input gas 80 % Ar + 20 % N₂ in a 200-A free-burning arc

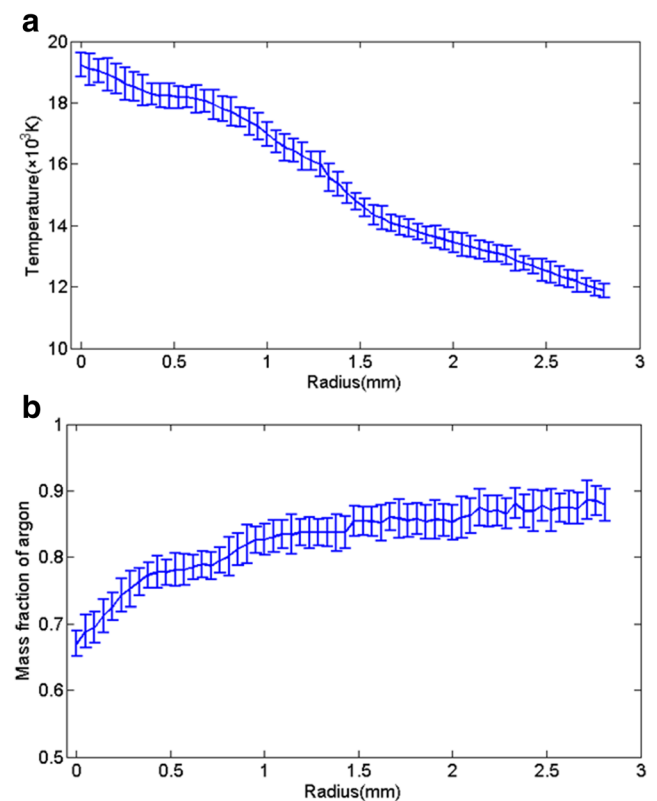


Fig. 8 Radial dependencies of **a** temperature and **b** mass fraction of argon measured 2 mm below the cathode tip with input gas 80 % Ar + 20 % N₂ in a 200-A free-burning arc, including the error bars of their values

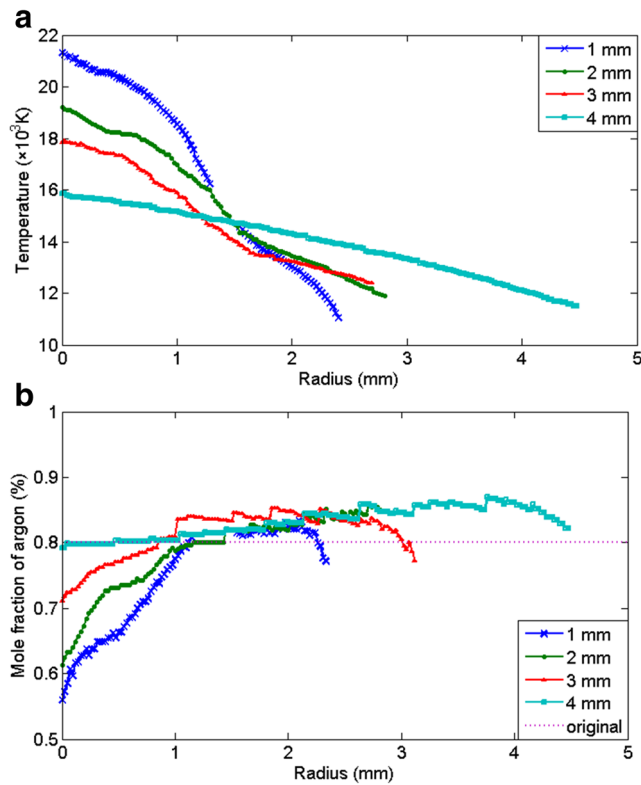


Fig. 9 Radial dependencies of **a** temperature and **b** mass fraction of argon measured 1, 2, 3, and 4 mm below the cathode tip with input gas 80 % Ar + 20 % N₂ in a 200-A free-burning arc

fraction of argon is lower than 80 % at the center of the arc plasma but increases at radii less than 2 mm. As the radius increases further, the argon mass fraction decreases again. This phenomenon may be associated with nitrogen molecule dissociation, which occurs when approaching the arc periphery at temperatures around 7000 K and causes an increase in the nitrogen mole fraction and consequently a decrease in the argon mole fraction. The mole fraction gradient causes the outward diffusion of argon toward this region.

The primary advantage of the monochromatic imaging method is that it allows for the analysis of the

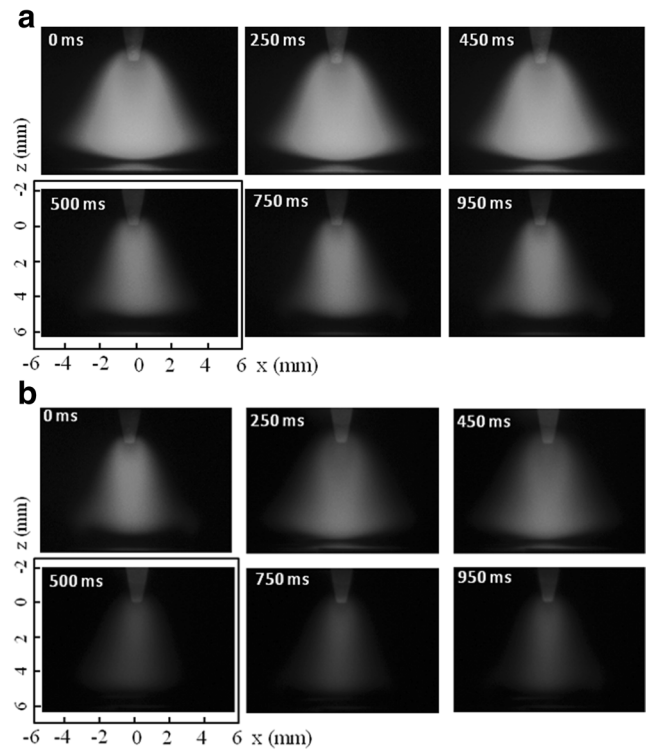


Fig. 10 Typical frames of the spectral intensity images of the **a** Ar I 794.8 nm line and **b** N I 904.6 nm line of P-TIG arc plasma ($I_p = 200$ A and $I_b = 100$ A) in a cycle after the welding process was stable. At the *top* are images (the first frame [0 ms], the middle frame [250 ms], and the last frame [450 ms]) in the peak-current phase, and at the *bottom* are images (the first frame [500 ms], the middle frame [750 ms], and the last frame [950 ms]) in the base-current phase

dynamic arc process. The temperature and composition of the P-TIG welding arc plasma are measured using the parameters in Table 1.

The intensity distributions of the Ar I 794.8 nm and N I 904.6 nm spectra are obtained after the welding process is stable to determine the plasma temperature and argon content. Figure 10a shows the six typical frames of Ar I 794.8 nm spectral intensity images in a cycle, and Fig. 10b shows the corresponding intensity images of N I 904.6 nm. On the top row of Fig. 10a, b are the images

Table 1 Welding parameters for P-TIG welding with Ar–N₂ shielding gas

Current		Frequency	Duty circle	Arc length	Gas flow rate	Tungsten diameter	Tungsten angle	Anode
I_p	I_b	Hz	%	mm	L/min	mm	deg	
200	100	1	50	5	10	2.4	60	Water-cooled copper

in the peak-current phase (i.e., the first frame [0 ms], the middle frame [250 ms], and the last frame [450 ms]), and on the bottom row are the images in the base-current phase (the first frame [500 ms], the middle frame [750 ms], and the last frame [950 ms]).

If the middle frame of Fig. 10a is taken as the typical example, the lateral profiles of the Ar I 794.8 nm intensities in the peak- and base-current phases at 2 mm below the cathode tip are as shown in Fig. 11a. The corresponding intensities of N I 904.8 nm are shown in Fig. 11b. Both the Ar I and N I intensities in the peak-current phase are higher than those in the base-current phase. The radial profiles of the plasma temperatures and concentrations are shown in Fig. 12. The temperature increases and the argon mass fraction decreases with an increasing radius in both the high- and low-current phases. The increase in temperature in the high-current phase, relative to the low-current phase, is larger in the argon–nitrogen arc plasma than in the pure argon arc plasma under the same experimental conditions.

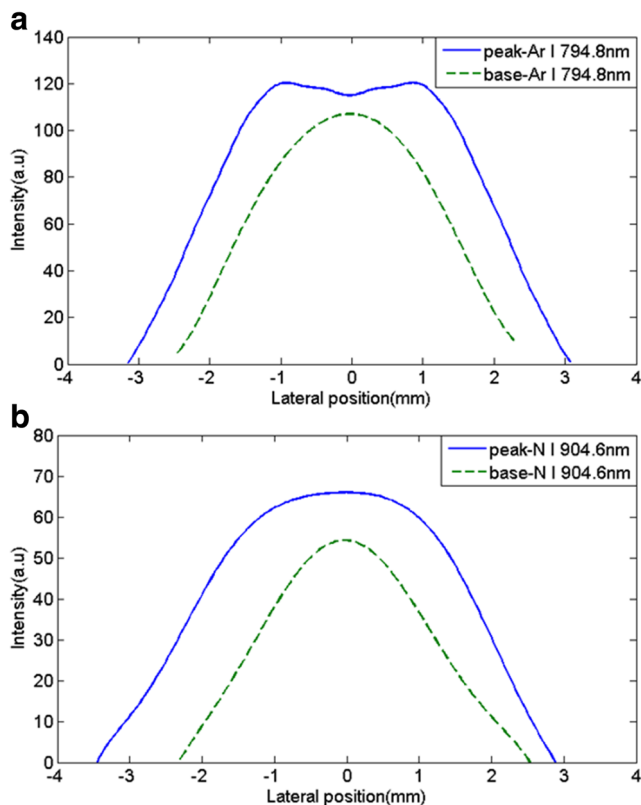


Fig. 11 Lateral distributions of **a** Ar I 794.8 nm and **b** N I 904.6 nm intensities measured 2 mm below the cathode tip of P-TIG welding ($I_p = 200$ A and $I_b = 100$ A) in 80 % Ar + 20 % N_2 arc plasma

The distributions of spectral line intensities as a function of time are presented in Fig. 13. The spectral line intensities are at the axial positions of the arc at distances of 1.0–4.0 mm from the cathode tip. The line intensity increases along the axial direction in the peak-current phase. The line intensity, which is the integral of the emission coefficient, is weak near the cathode tip, because the emission coefficient has an off-axis maximum value. Subsequently, it increases as the diameter expands. However, the intensity variation in the base-current phase is not significant, because the Ar I 794.8 nm and N I 904.6 nm intensities are relatively low and difficult to compare.

The plasma temperatures and compositions can then be determined using the modified Fowler–Milne method, as shown in Fig. 14. The temperatures and argon mass fractions vary periodically with the current. A higher current in the peak-current phase results in a higher temperature near the arc axis and consequently larger temperature gradients. Demixing is therefore stronger in the peak-current phase; as a result, the mass fraction of argon near the arc axis is lower.

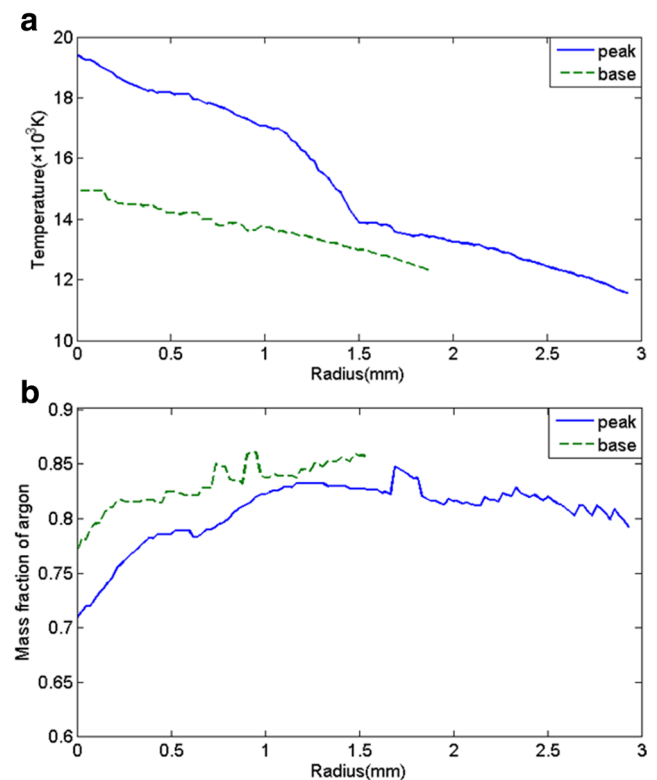


Fig. 12 Radial dependencies of **a** temperature and **b** mass fraction of argon measured 2 mm below the cathode tip of P-TIG welding ($I_p = 200$ A and $I_b = 100$ A) in the 80 % Ar + 20 % N_2 arc plasma

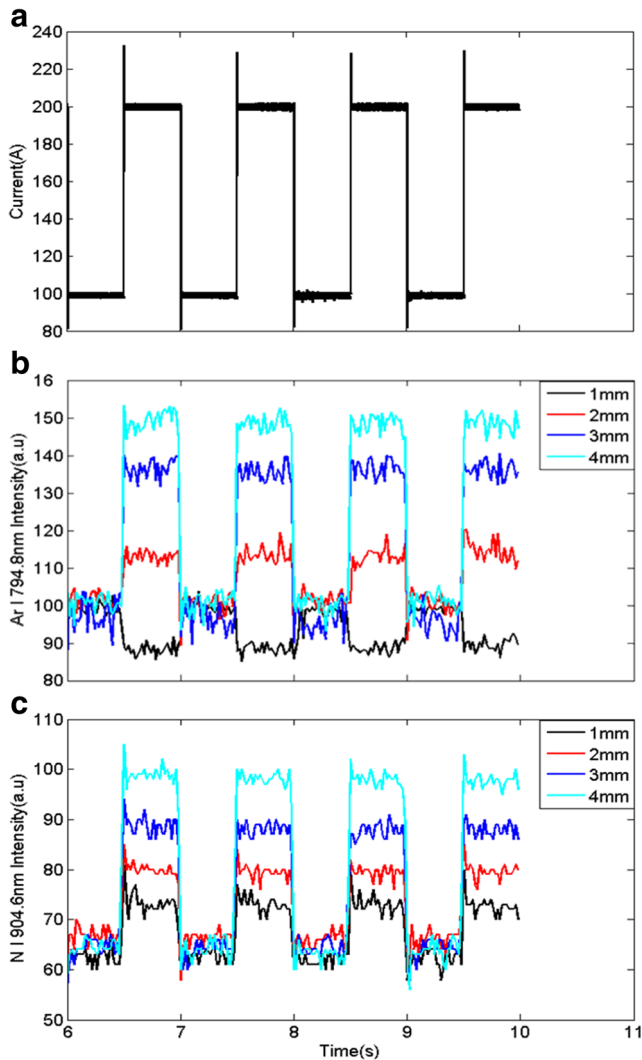


Fig. 13 Change characteristics of **a** current, **b** Ar I 794.8 nm intensity, and **c** N I 904.6 nm intensity at various axial positions (1, 2, 3, and 4 mm) of P-TIG welding ($I_p = 200$ A and $I_b = 100$ A) in 80 % Ar + 20 % N₂ arc plasma

5 Conclusion

The arc image acquisition system was developed to capture monochromatic images of Ar I and N I in the argon–nitrogen arc plasma, and the modified Fowler–Milne method was used to determine the temperature and gas composition of this arc plasma in both DC-TIG and P-TIG welding. The following conclusions were drawn:

- The arc image acquisition system contains two monochromatic image devices, and they are triggered synchronously by a software program. Each of the monochromatic image

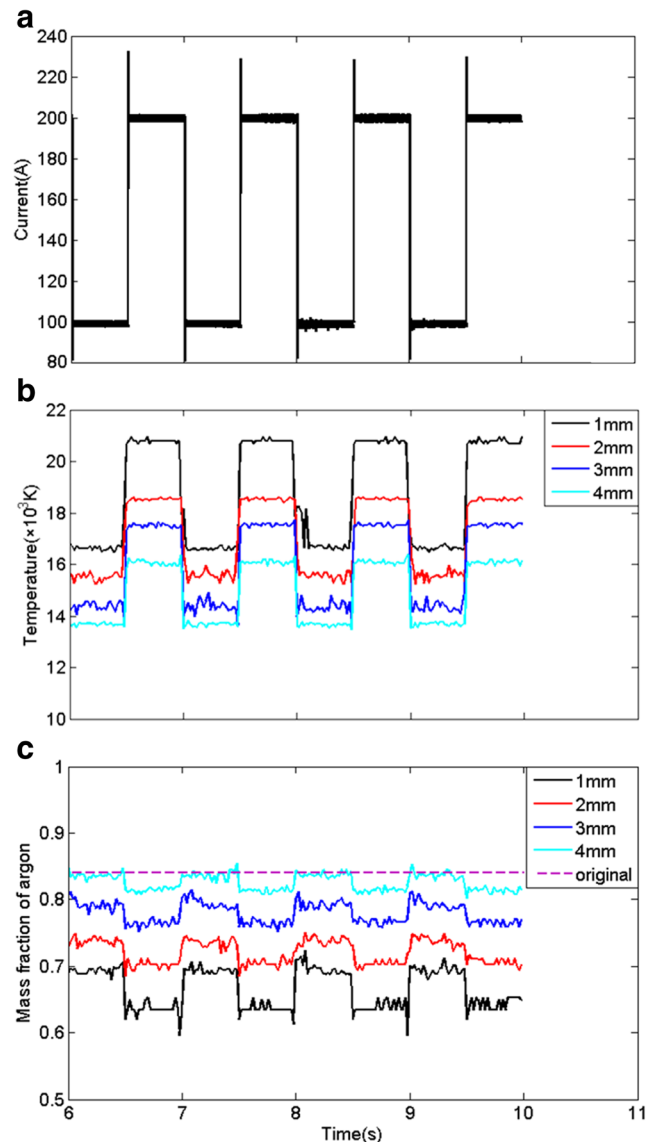


Fig. 14 Change characteristics of **a** current, **b** temperature, and **c** concentration distributions at various axial positions (1, 2, 3, and 4 mm) in the 80 % Ar + 20 % N₂ arc in P-TIG welding

devices consists of a camera lens, neutral density filters, a narrow bandpass filter, and a CCD sensor.

- In DC-TIG welding using 80 % Ar + 20 % N₂ shielding gas, the temperature of the gas mixture is higher than that of pure argon under the same condition; as a result, the thermal transport to the workpiece is enhanced. Demixing causes a change in the composition distribution. The concentration of argon in the arc center is lower than that in the original gas mixture, and it gradually increases with the radius as a consequence of the frictional forces. It

begins to decrease after it reaches a peak value because of the diffusion of argon atoms.

- For P-TIG welding using 80 % Ar + 20 % N₂ mixture, the temperatures and gas compositions vary periodically with current. A higher current in the peak-current phase results in a higher temperature near the arc axis and consequently larger temperature gradients. Demixing is therefore stronger in the peak-current phase; as a result, the mass fraction of argon near the arc axis is lower.
- The established system is simple, stable, and rapid. The method can be used to determine the temperatures and gas compositions of either static or dynamic plasmas. This study provides experimental data to verify simulation results.

Acknowledgments The authors acknowledge support from the National Natural Science Foundation of China; the grant number is 51275299.

References

1. Liu Zhanmin LM (2005) Analysis of Ar-N arc behavior and copper plate welding. *Weld Join* 49(10):20–23
2. Lothongkum G, Viyanit E, Bhandhubanyong P (2001) Study on the effects of pulsed TIG welding parameters on delta-ferrite content, shape factor and bead quality in orbital welding of AISI 316L stainless steel plate. *J Mater Process Technol* 110(2):233–238
3. Murphy A (1997) Demixing in free-burning arcs. *Phys Rev E* 55(6):7473
4. Thornton M (1993) Spectroscopic determination of temperature distributions for a TIG arc. *J Phys D Appl Phys* 26(9):1432
5. Yu H et al. (2013) Arc spectral processing technique with its application to wire feed monitoring in Al–Mg alloy pulsed gas tungsten arc welding. *J Mater Process Technol* 213(5):707–716
6. Ma S et al. (2011) Spectroscopic measurement of temperatures in pulsed TIG welding arcs. *J Phys D Appl Phys* 44(40):405202
7. Ma S, Gao H, Wu L (2008) Spatial spectroscopic diagnostics of arc plasmas by monochromatic imaging. *Plasma Sci, IEEE Trans* 36(4):1054–1055
8. Ma S, Gao H, Wu L (2011) Time resolved characterization of a free-burning argon arc after ignition by optical emission spectroscopy. *J Appl Phys* 110(2):026102
9. Sawato H et al. (2011) Measurement of dynamical variation in two-dimensional temperature distribution of TIG pulsed-arcs. *Proc Japan Weld Inst* 29:23s–26s
10. Xiao X et al. (2014) A modified Fowler–Milne method for monochromatic image analysis in multi-element arc plasma welding. *J Mater Process Technol* 214(11):2770–2776
11. Song Y (1990) Research on spectroscopic diagnosis and application of welding arc plasma[D]. Tianjin University, Tianjin
12. Li H, Li J, Li Y (1993) High thermal characteristic of argon-nitrogen TIG arc. *Weld J* 14(2):125–130
13. Hiraoka K (1993) Evaluation of local plasma composition and temperature in mixed gas tungsten arc plasma column by light spectroscopy—study on characteristics of gas tungsten arc shielded by mixed gases (report 2). *Q J Jpn Weld Soc* 11(1):68–74
14. Hiraoka K (1998) Plasma structures of Ar-H₂ mixed gas tungsten arcs determined by spectroscopic measurements. *Weld Int* 12(3):186–194
15. Hiraoka K, Shiwaku T, Ohji T (1997) Determining temperature distributions of gas tungsten arc (TIG) plasma by spectroscopic methods. *Weld Int* 11(9):688–696
16. Murphy AB (1994) Modified Fowler–Milne method for the spectroscopic measurement of temperature and composition of multi-element thermal plasmas. *Rev Sci Instrum* 65(11):3423
17. Xiao X, Hua X, Wu Y (2015) Comparison of temperature and composition measurement by spectroscopic methods for argon-helium arc plasma. *Opt Laser Technol* 66:138–145
18. Farmer A, Haddad G, Cram L (2000) Temperature determinations in a free-burning arc. III. Measurements with molten anodes. *J Phys D Appl Phys* 19(9):1723
19. Bockasten K (1961) Transformation of observed radiances into radial distribution of the emission of a plasma. *JOSA* 51(9):943–947
20. Lancaster JF (1984) The physics of welding. *Phys Technol* 15(2):73